Evolution and stability of self-localized modes in a nonlinear inhomogeneous crystal lattice

A. D. Boardman
Department of Physics, Joule Laboratory, University of Salford, Salford M5 4WT, United Kingdom

V. Bortolani
Department of Physics, University of Modena, Modena, Italy

R. F. Wallis
Department of Physics and Institute for Surface and Interface Science, University of California, Irvine, California 92717

K. Xie and H. M. Mehta
Department of Physics, Joule Laboratory, University of Salford, Salford M5 4WT, United Kingdom
(Received 23 January 1995; revised manuscript received 19 May 1995)

The evolution and stability of self-localized modes in an inhomogeneous crystal lattice are discussed. After establishing the basic equations, appropriate time and space scales are introduced, together with a power threshold. A mathematical stability theory, based upon an averaged Lagrangian analysis, concludes that the system is stable for any mass defect, if the perturbation is symmetric. For asymmetric perturbations, only single-peaked stationary states are stable. Finally, numerical simulations are presented that not only support the theoretical work of the earlier sections but show clearly the evolution of the solutions from a range of input conditions.

I. INTRODUCTION

Investigations of anharmonic effects on atomic vibrations in crystals have increased considerably in recent years. Of particular interest are studies of strongly anharmonic crystals which demonstrate the existence of localized modes with frequencies above the maximum frequency of the harmonic crystal. These modes, which exist in perfect lattices, are strongly localized about a particular lattice site. This site can be chosen to be any lattice site because of translational invariance. Sievers and Takeno[1] have used the term intrinsic localized modes (ILM's) to distinguish them from defect-induced localized modes. Another term which has been used[2] is self-localized anharmonic modes (SLAM's).

An early discussion of ILM's was presented by Kosevich and Kovalev[3] who employed the continuum approximation to the equations of motion. The latter were assumed to contain cubic and quartic anharmonic terms, in addition to harmonic terms. Solutions were obtained that correspond to envelope solitons whose spatial extent is large compared to the lattice constant. Somewhat later, Dolgov[4] treated the problem by solving the equations of motion for a monatomic linear chain with nearest neighbor harmonic and quartic anharmonic interactions. He found ILM's of both even and odd parity. Further work on the odd-parity ILM's has been reported by Sievers and Takeno[1] and on the even-parity ILM's by Page[5] and Takeno.[6] Cubic anharmonicity has been shown by Bickham, Kiselev, and Sievers[7] to lower the frequency of an ILM and to be accompanied by amplitude-dependent static distortions. Diatomic linear chains have been investigated by Kiselev, Bichkham, and Sievers[8] using two-body potentials, such as those of Morse and Lennard-Jones. An ILM was found with its frequency in the forbidden gap between the acoustic and optical branches but no ILM was found with frequency above the top of the optical branch. Kivshar[9] has studied an ILM localized at an impurity atom. When the impurity mass is larger than that of the host atoms, the ILM has double maxima, otherwise it has a cusped maximum. In both the cases, when the impurity mass is larger, or less, than that of the host atoms, the envelope of the ILM has a discontinuity of slope.[9]

This paper discusses the modes localized at an impurity atom. The basic dynamical equations, and the route to a modified nonlinear envelope Schrödinger equation, are quickly established. The solutions proposed by Kivshar[9] are then highlighted but useful linear and nonlinear times scales are introduced to cast the envelope equation into dimensionless form. In this way, it is easy to see the magnitudes of the spatial and time scales, over which the localized modes develop. It is also straightforward to produce an amplitude threshold for the effect.

A perturbation theory, resting upon an averaged Lagrangian technique, is then developed, in which a multiparameter trial function is introduced. The resulting reduced Lagrangian enables the reduced Hamiltonian to be picked out and hence an effective potential energy function to be defined. The second derivative of this function immediately reveals a mathematical condition for the stability of the nonlinear system.

Finally, a full numerical simulation is presented which demonstrates the existence of the single and double peaked stationary states. The numerical work also completely supports the mathematical conclusions that were obtained from the Lagrangian analysis.

II. LATTICE DYNAMICAL EQUATIONS OF MOTION AND SOLUTIONS

The vibrations of a monatomic linear chain of atoms, with mass m, are considered. Each atom interacts only with its

nearest neighbors via an interaction potential consisting of harmonic and quartic anharmonic terms with force constants k_2 and k_4, respectively. The equations of motion are

$$m\ddot{u}_n = k_2(u_{n+1}+u_{n-1}-2u_n) + k_4[(u_{n+1}-u_n)^3+(u_{n-1}-u_n)^3], \quad (1)$$

where u_n is the displacement of the nth atom. Note that here the cubic force constant, k_3, is omitted. The investigations of Bickham, Kiselev, and Sievers[7] show that self-localized vibrational modes are stable, however, even for large cubic anharmonicities. Hence, although the frequencies of stationary modes are actually a function of k_3, for a given k_4, the effect of finite k_3 on the localized modes studied here is considered to be small.[7]

In the harmonic approximation, for which $k_4=0$, the solutions to Eq. (1) for an infinite chain can be written as $u_n = A\exp[i(kan-\omega t)]$, where k is the wave number, a is the lattice constant, and ω is the angular frequency given by $\omega=\omega_m \sin(ka/2)$. The maximum frequency ω_m is $2(k_2/m)^{1/2}$. If quartic anharmonicity is switched on, ILM's can exist at any lattice site provided the anharmonicity is sufficiently strong.[1] The frequency of the odd-parity ILM is given, within the rotating wave approximation, by

$$\omega \approx \left[\frac{3\omega_m^2}{4}\left(1+\frac{27k_4A^2}{16k_2}\right)\right]^{1/2} \quad (2)$$

and this must be greater than ω_m. The displacement pattern is approximated by u_n: $A(\ldots,0,-\frac{1}{2},1,-\frac{1}{2},0)$.

If an anisotropic impurity of mass M is introduced at the lattice site $n=0$, the equations of motion are Eq. (1) appended by $(m-M)\ddot{u}_n\delta_{n0}$, where δ_{n0} is the Kronecker delta. In the harmonic approximation a localized impurity mode exists[10] if $M<m$ and has a frequency greater than ω_m, given by

$$\omega^2 = \frac{\omega_m^2}{\frac{M}{m}\left(2-\frac{M}{m}\right)} \approx 2k_2\left(\frac{1}{M}+\frac{1}{2m}\right). \quad (3)$$

When quartic anharmonicity is included, the frequency of the localized mode is approximately[9]

$$\omega^2 \approx 2k_2\left(\frac{1}{M}+\frac{1}{2m}\right)+\frac{3}{2}k_4A^2\left(1+\frac{M}{2m}\right)^3, \quad (4)$$

and the displacement pattern is u_n: $A(\ldots,0,-(M/2m),1,-(M/2m),0,\ldots)$.

Kivshar[9] treated the impurity problem in the continuum limit and obtained the envelope soliton solution

$$\psi(x,t) = \frac{A\exp(i\Omega t)}{\cosh[B(|x|-x_0)]}, \quad (5)$$

where $B^2=6k_4A^2/a^2k_2$, $\Omega=(3/4)\omega_m k_4A^2/k_2$, and x_0 is specified by

$$aB\tanh(Bx_0) = -2(m-M)/m. \quad (6)$$

For $M<m$, x_0 is negative and the mode profile is similar to that in the linear case with $\psi(x,t)$ having a maximum at the impurity site. For $M>m$, however, x_0 is positive and the impurity mode has two maxima at $x=\pm x_0$.

III. THE MODIFIED NONLINEAR SCHRÖDINGER EQUATION AND ITS SOLUTIONS

The lattice displacement $u_n(t)$ is assumed to have the form

$$u_n(t) = \frac{1}{2}(-1)^n\psi_n(t)e^{i\omega_m t}+\text{c.c.} \quad (7)$$

Note that, in Eq. (7), the *fast* time variation is factored as $e^{i\omega_m t}$, leaving $\psi_n(t)$ as a *slowly* varying function. This, so-called, slowly varying envelope approximation permits the neglect of $\ddot{\psi}_n$, in comparison with $\dot{\psi}_n$. For a chain of atoms, with a site label n and an interatomic distance a, a continuous variable $x=na$ can now be introduced to cast the equation for $\psi_n(t)$ into an envelope equation for $\psi(x,t)$. The transformation from the lattice equations of motion to a differentiable equation for $\psi(x,t)$ can be effected by setting

$$\psi_{n\pm1} \approx \psi(x,t) \pm a\frac{\partial\psi(x,t)}{\partial x}+\frac{a^2}{2}\frac{\partial^2\psi(x,t)}{\partial x^2}. \quad (8)$$

If an isotopic impurity exists at a lattice site then the Kronecker δ_{n0} becomes the delta function $\delta(x)$ and the final, modified, form of the nonlinear Schrödinger equation is[9]

$$2i\omega_m\frac{\partial\psi}{\partial t}+\frac{a^2k_2}{m}\frac{\partial^2\psi}{\partial x^2}+\frac{12k_4}{m}|\psi|^2\psi = -a\omega_m^2\mu\delta(x)\psi, \quad (9)$$

where $\mu=m-M/m$ is the mass defect parameter.

There are a number of ways now to introduce characteristic times, or lengths, in order to turn the nonlinear Schrödinger into a dimensionless, generic, form.[11] The method chosen here introduces characteristic times t_D and $t_{\rm NL}$, which are defined through the following arguments. The fundamental stationary state solution of the homogeneous equation has a hyperbolic secant form, with respect to the variable x, and $|u|$ will remain constant in shape as time, t, elapses. Any initial condition, such as a Gaussian shape, will, provided a certain threshold amplitude is exceeded, for a given half-width, evolve in time to the hyperbolic secant soliton form. For the lowest initial energies, this is done by shedding unwanted energy until the stationary state is achieved. If the nonlinearity is not sufficiently strong to contain the localized mode in the x direction then it will delocalize (spread) and will do so with a characteristic time $t_D=2[D_0^2m\omega_m]/(a^2k_2)$, which is roughly twice the time taken for an initial Gaussian-like pulse with a width D_0 to double its size. If the amplitude ψ is $\psi_m u$, where ψ_m is the maximum amplitude, and u is now dimensionless, then a nonlinear time $t_{\rm NL}=(m\omega_m)/(3k_4\psi_m^2)$ can also be defined. In the absence of the "spreading" term $(a^2k_2/m)\psi_{xx}$, the solution of Eq. (9) is $\psi=\psi(x,0)e^{i\phi(x,t)}$, where $\phi(x,t)=2(t/t_{\rm NL})$. Hence, $t_{\rm NL}/2$ is the time that elapses for the nonlinear phase shift to become 1. If t is now measured in units of t_D, x in units of D_0, and ψ in units of ψ_m, then the nonlinear Schrödinger equation becomes

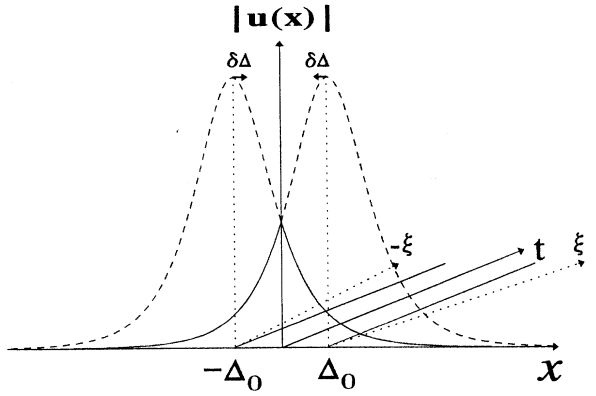

FIG. 1. Sketch of the stationary state solutions. Perturbations $\delta\Delta$ and ξ are also indicated on the figure.

$$i\frac{\partial u}{\partial t}+\frac{\partial^2 u}{\partial x^2}+2\frac{t_D}{t_{\mathrm{NL}}}|u|^2u=2\mu\delta(x)u, \tag{10}$$

where $t=t_Dt'$, $x=D_0x'$, $\mu'=-\frac{1}{2}(m\omega_m^2D_0/ak_2)\mu$, and the dashes have been dropped for notational simplicity. The ratio

$$\frac{t_D}{t_{\mathrm{NL}}}=\frac{6D_0^2k_4\psi_m^2}{a^2k_2} \tag{11}$$

is an interesting quantity, because it must be unity for Eq. (10) to possess exactly the lowest-order soliton (hyperbolic secant) solution. The ratio shows that, for a homogeneous lattice and a given D_0, the threshold condition for the lowest stationary state is

$$\psi_m^2=\frac{a^2}{6}\frac{k_2}{k_4}\frac{1}{D_0^2}. \tag{12}$$

The solution of Eq. (10), for $t_D/t_{\mathrm{NL}}=1$, is $u=\mathrm{sech}(|x|-x_0)e^{it}$, where $x_0=\tanh^{-1}(\mu)$ locates the peak of the function, which is a dimensionless form of the one derived by Kivshar.[9] The x-dependent part of the solution, $|u|$, is sketched in Fig. 1, where the solid curve corresponds to $\mu<0$, and the two-humped dashed curve corresponds to $\mu>0$.

The discontinuity in du/dx is clearly in evidence at $x=0$. The mathematical solutions of the modified nonlinear Schrödinger equation are interesting but it remains to be seen whether they are stable for all μ. It is also important to study the evolution of these solutions from various input conditions.

IV. STABILITY OF THE SOLUTIONS

For $t_D/t_{\mathrm{NL}}=1$, Eq. (10), through the application of the Euler-Lagrange equations, comes from the Lagrangian density

$$L=\frac{i}{2}\left[u^*\frac{\partial u}{\partial t}-u\frac{\partial u^*}{\partial t}\right]-\left|\frac{\partial u}{\partial x}\right|^2+|u|^4-2u\,\delta(x)|u|^2 \tag{13a}$$

and the corresponding Hamiltonian density is

$$H=\left|\frac{\partial u}{\partial x}\right|^2-|u|^4+2u\,\delta(x)|u|^2. \tag{13b}$$

The stationary solution of Eq. (10) is, in a more general form,

$$u(x,t)=\rho_0\mathrm{sech}[\rho_0|x|-\Delta_0]e^{i\rho_0^2t}, \tag{14}$$

where Δ_0 satisfies $\rho_0\tanh(\Delta_0)=\mu$.

Note that here an amplitude ρ_0 has been introduced and that ρ_0 is also the reciprocal of the half-width, as it is required to be for a solitonlike, localized, solution. $\rho_0=1$ reduces Eq. (14) to the solution previously discussed. The single peak solution occurs for $\Delta_0<0$ and the double peak solution occurs for $\Delta_0>0$. The use of ρ_0 here is to introduce the amplitude, specifically, and then to determine how this evolves in time, in response to a perturbation.

If the solution (14) is perturbed it will take the form

$$x>0: u_+=\eta_2\mathrm{sech}[\rho_2x-\Delta_2]\exp\left[\frac{i\xi_2}{2\rho_2}(\rho_2x-\Delta_2)+\frac{iC_2}{2\rho_2^2}(\rho_2x-\Delta_2)^2+i\rho_0^2t\right], \tag{15a}$$

$$x<0: u_-=\eta_1\mathrm{sech}[\rho_1x+\Delta_1]\exp\left[\frac{i\xi_1}{2\rho_1}(\rho_1x+\Delta_1)-\frac{iC_1}{2\rho_1^2}(\rho_1x+\Delta_1)^2+i\rho_0^2t\right], \tag{15b}$$

where the $\xi_{1,2}$ are analogous to velocity and $C_{1,2}$ are spatial phase changes, called *chirp* in nonlinear optics and radar physics. The boundary conditions

$$\left[\frac{du}{dx}\right]_{-0}^{+0}=2\mu u(0);\quad u(+0)=u(-0) \tag{16}$$

lead to the relationships

$$\eta_2\mathrm{sech}(\Delta_2)=\eta_1\mathrm{sech}(\Delta_1), \tag{17a}$$

$$\rho_2\tanh(\Delta_2)+\rho_1\tanh(\Delta_1)=2\mu, \tag{17b}$$

$$\frac{\xi_2}{2}-\frac{C_2}{\rho_2}\Delta_2=\frac{\xi_1}{2}-\frac{C_1}{\rho_1}\Delta_1, \tag{17c}$$

$$-\frac{\xi_2}{\rho_2}\Delta_2+\frac{C_2}{\rho_2^2}\Delta_2^2=\frac{\xi_1}{\rho_1}\Delta_1-\frac{C_1}{\rho_1^2}\Delta_1^2. \tag{17d}$$

If the energy conservation is expressed as

$$\int_{-\infty}^{\infty}|u|^2dx=2E, \tag{18}$$

then

$$\frac{\eta_1^2}{\rho_1}[\tanh(\Delta_1)+1]+\frac{\eta_2^2}{\rho_2}[1+\tanh(\Delta_2)]=2\rho_0[1+\tanh(\Delta_0)]$$
$$=2E. \tag{19}$$

Following Whitham's method,[12] the Lagrangian density L is averaged, by integrating over x, as a prelude to determining how the parameters in solutions (15) vary as the localized excitation develops. The averaged Lagrangian is

$$\mathscr{L}=\int_{-\infty}^{\infty} L\,dx=\mathscr{L}_+ +\mathscr{L}_-,$$

where

$$\begin{aligned}\mathscr{L}_+ =-\Bigg(&-\frac{1}{2}\frac{\Delta_2}{\rho_2}\frac{\partial\xi_2}{\partial t}-\frac{1}{2}\frac{\xi_2}{\rho_2}\frac{\partial\Delta_2}{\partial t}+\frac{1}{2}\frac{\xi_2\Delta_2}{\rho_2^2}\frac{\partial\rho_2}{\partial t}+\frac{1}{2}\frac{\Delta_2^2}{\rho_2^2}\frac{\partial C_2}{\partial t}\\&+\frac{C_2\Delta_2}{\rho_2^2}\frac{\partial\Delta_2}{\partial t}-\frac{C_2\Delta_2^2}{\rho_2^3}\frac{\partial\rho_2}{\partial t}+\rho_0^2-\frac{\xi_2^2}{4}-\frac{C_2}{\rho_2^2}\Delta_2^2+\frac{\xi_2C_2\Delta_2}{\rho_2}+\eta_2^2\Bigg)\frac{\eta_2^2}{\rho_2}[1+\tanh(\Delta_2)]\\&-\left(\frac{1}{2}\frac{\partial\xi_2}{\partial t}-\frac{C_2}{\rho_2}\frac{\partial\Delta_2}{\partial t}-\frac{\Delta_2}{\rho_2}\frac{\partial C_2}{\partial t}+\frac{C_2\Delta_2}{\rho_2^2}\frac{\partial\rho_2}{\partial t}-\xi_2C_2+\frac{2C_2^2\Delta_2}{\rho_2}\right)\frac{\eta_2^2}{\rho_2^2}[\ln\cosh(\Delta_2)+\Delta_2+\ln 2]\\&-\left(\frac{1}{2}\frac{\partial C_2}{\partial t}+C_2^2\right)\frac{\eta_2^2}{\rho_2^3}F(\Delta_2)-\frac{\eta_2^2}{3\rho_2}[\rho_2^2+\eta_2^2][1+\tanh^3(\Delta_2)]-\mu\eta_2^2\operatorname{sech}^2(\Delta_2),\end{aligned} \tag{20}$$

where $(F(\Delta_2)=\int_0^\infty x^2\operatorname{sech}^2(x-\Delta_2)dx$, and $\mathscr{L}_-$ is generated by replacing Δ_2 by Δ_1, ξ_2 by $-\xi_1$, ρ_2 by ρ_1, η_2 by η_1, and C_2 by $-C_1$.

Symmetric perturbation

The aim now is to discover whether solutions are stable for all μ, or only for one sign of μ. This will be important information showing whether both the single peak ($\mu<0$) and the double peak ($\mu>0$) solutions are both stable with respect to symmetric perturbations. A symmetric perturbation will be defined as (see Fig. 1)

$$\Delta_1=\Delta_2=\Delta=\Delta_0+\delta\Delta,\quad -\xi_1=\xi_2=\xi,\quad -C_1=C_2=C,$$
$$\rho_1=\rho_2=\rho,\quad \eta_1=\eta_2=\eta.$$

These conditions simplify the conditions (17) and (19) to

$$C=\frac{\xi\rho}{2\Delta},\quad \rho=\frac{\mu}{\tanh(\Delta)},$$
$$\eta^2=\frac{1+\tanh(\Delta_0)}{1+\tanh(\Delta)}\rho_0\rho=\frac{\rho}{1+\tanh(\Delta)}E. \tag{21}$$

For this symmetric perturbation, $\mathscr{L}_+=\mathscr{L}_-\equiv\mathscr{L}$ so the reduced Hamiltonian is

$$\mathscr{H}=\mu\rho[1-\tanh(\Delta)]E-\eta^2E+\frac{1}{3}(\eta^2+\rho^2)$$
$$\times[1-\tanh(\Delta)+\tanh^2(\Delta)]E+\frac{\eta^2F}{4\rho\Delta^2}\xi^2 \tag{22}$$

from which a potential function U can be easily identified. If the constant E is absorbed into U, then after some labor,

$$U=\frac{\mu^2}{3}\left[\frac{1}{\tanh(\Delta_0)}-\frac{1}{\tanh^2(\Delta)}-\frac{2}{\tanh(\Delta)\tanh(\Delta_0)}-1\right]. \tag{23}$$

The stationary point of U is at $\tanh(\Delta)=\tanh(\Delta_0)$ and the second derivative is

$$\left[\frac{\partial^2U}{\partial(1/\tanh\Delta)^2}\right]_{\Delta_0}=\frac{2}{3}\mu^2\geq 0. \tag{24}$$

Hence the localized states are stable for all μ.

Asymmetric perturbation

For this type of perturbation

$$\xi_1=\xi_2=\xi,\Delta_1=\Delta_0-\delta\Delta,\Delta_2=\Delta_0+\delta\Delta$$

and the relationships (17) simplify to

$$\eta_1=\rho_1=\frac{2\mu\cosh(\Delta_1)}{\sinh(\Delta_1)+\sinh(\Delta_2)}, \tag{25a}$$

$$\eta_2=\rho_2=\frac{2\mu\cosh(\Delta_2)}{\sinh(\Delta_1)+\sinh(\Delta_2)}, \tag{25b}$$

$$C_1=\frac{\rho_1}{\Delta_1}\xi,\quad C_2=\frac{\rho_2}{\Delta_2}\xi. \tag{25c}$$

These new relationships satisfy both the boundary conditions and energy conservation. The reduced Hamiltonian $\mathscr{H}_+$ can easily be picked out from (20) and then manipulated by (25) to

$$\mathscr{H}_+ = \frac{\rho_2^3}{3}[3+\tanh(\Delta_2)-2\ \tanh^3(\Delta_2)-1]-\mu\rho_2^2\mathrm{sech}^2(\Delta_2)$$
$$+\xi^2\rho_2\left[-\frac{1}{4}\tanh(\Delta_2)+\frac{1}{\Delta_2}\ln[2\ \cosh(\Delta_2)]\right.$$
$$\left.+\frac{3}{4}-\frac{1}{\Delta_2^2}F(\Delta_2)\right]. \quad (26)$$

$\mathscr{H}_-$ is generated by the transformations $\rho_2\rightarrow\rho_1$, $\Delta_2\rightarrow\Delta_1$. The potential function is

$$U=\frac{\rho_2^3}{3}[2\ \tanh^3(\Delta_2)-3\ \tanh(\Delta_2)-1]$$
$$+\frac{\rho_1^3}{3}[2\ \tanh^3(\Delta_1)-3\ \tanh(\Delta_1)-1]$$
$$+\mu[\rho_2^2\mathrm{sech}^2(\Delta_2)+\rho_1^2\mathrm{sech}^2(\Delta_1)]. \quad (27)$$

The second derivative of U with respect to $\delta\Delta$, evaluated at Δ_0, is

$$\left[\frac{d^2U}{d(\delta\Delta)^2}\right]_{\Delta_0}=-\rho_0\mu(\rho_0+\mu) \quad (28)$$

but, $\mu=\rho_0\tanh(\Delta_0)$ so that $(\rho_0+\mu)>0$. Hence

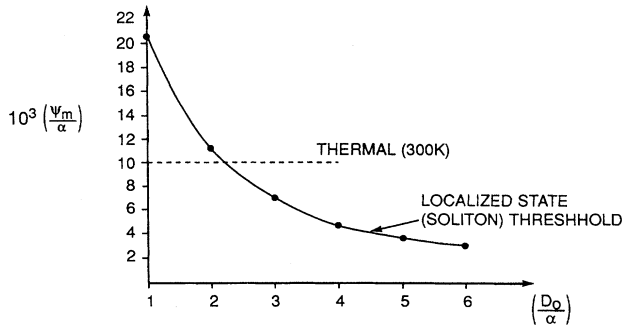

FIG. 2. Variation of localized state (soliton) threshold with (D_0/a). The dotted line gives the thermal value of the root mean square displacement.

$$\left[\frac{d^2U}{d(\delta\Delta)^2}\right]_{\Delta_0}\begin{cases}>0, & \mu<0\\ <0, & \mu>0\ .\end{cases} \quad (29)$$

This result means that, for an antisymmetric perturbation the single peak solution is stable, while the double peak structure is unstable. The overall conclusion is that the single peak bound state is always stable and that the double peak is only stable with respect to symmetric perturbations. This conclusion, regarding the double peak case, is a modification of the conclusion drawn by Kivshar that this stationary

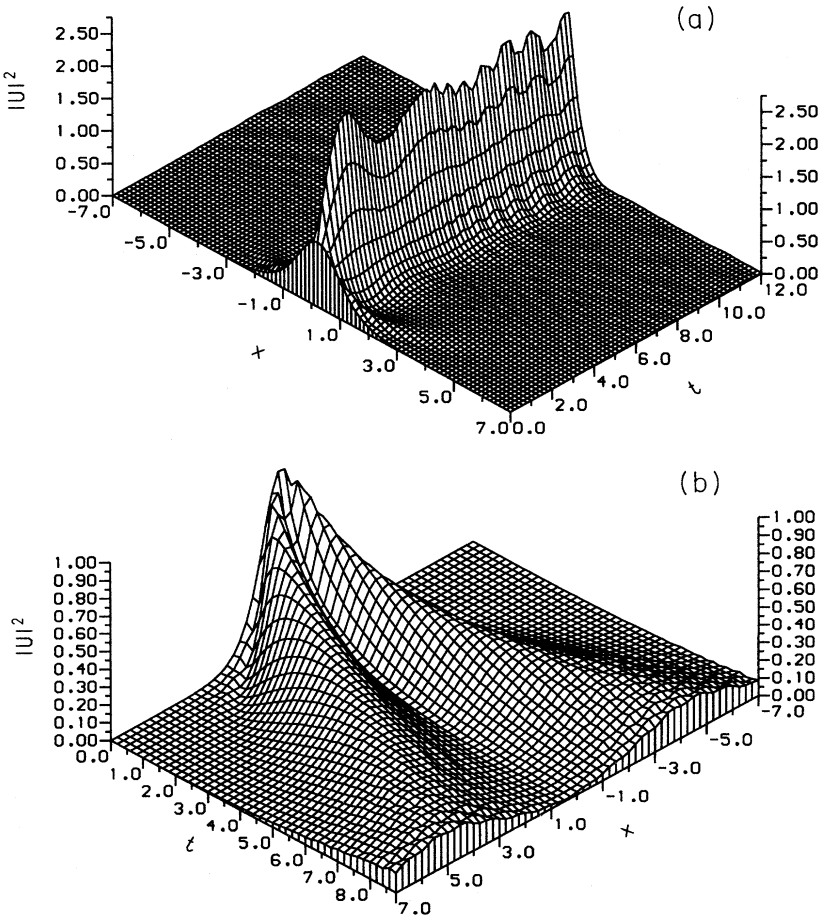

FIG. 3. Evolution of the nonlinear localized modes with time, for various input functions at $t=0$. The transverse x scale is measured in units of $D_0=4a=1.6$ nm and the time scale is in units of $(D_0^2 m\omega_m)/(a^2k_2)=0.16$ ps. (a) Evolution towards the sharp, single peak, stationary state, from a sech(x) input, for $\mu=-0.89$. (b) An attempt to evolve the double peak state from a sech(x) input, for $\mu=0.89$.

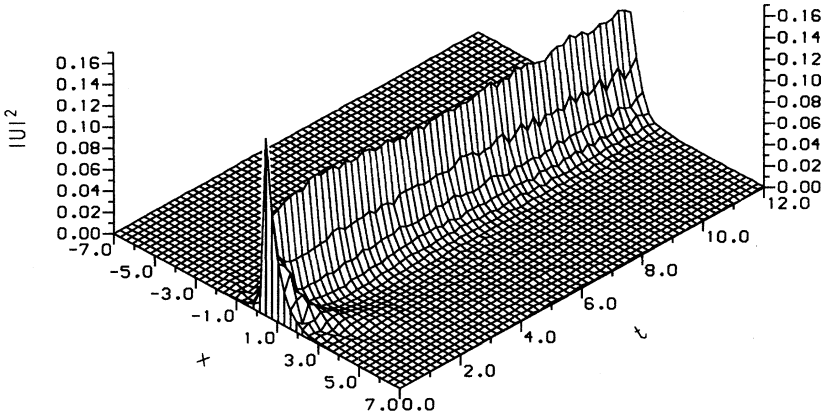

FIG. 4. Evolution of an asymmetric perturbation of the single-peak localized mode for the lattice data of Fig. 3. $\mu=0.89$ and the input function is $[\mathrm{sech}(x-x_1),\ x>0]$, $[\mathrm{sech}(x-x_2),\ x<0]$, where $x_1=0.95\ \tanh^{-1}(\mu)$ and $x_2=1.05\ \tanh^{-1}(\mu)$.

state is always unstable.[9] The main features of the simple result quoted by Kivshar[9] can easily be obtained from the work reported here by setting $\rho_1=\rho_2=\rho_0$, $\mu\to-2\mu'$ and $\Delta_2\approx\delta\Delta,\Delta_1\approx-\delta\Delta$. These assumptions are consistent with $|\mu|\ll 1$ and lead to

$$U\approx-2\mu'\rho_0^2\mathrm{sech}^2(\delta\Delta)-\tfrac{2}{3}\rho_0^3. \tag{30}$$

If the ρ_0^3 terms are absorbed in U then a new potential U' can be defined where

$$U'=\frac{-2\mu'\rho_0^2}{\cosh^2(\delta\Delta)} \tag{31}$$

which would lead to the conclusion that the potential is repulsive for $\mu'<0$ $(\mu>0)$ and instability *always* ensues, no

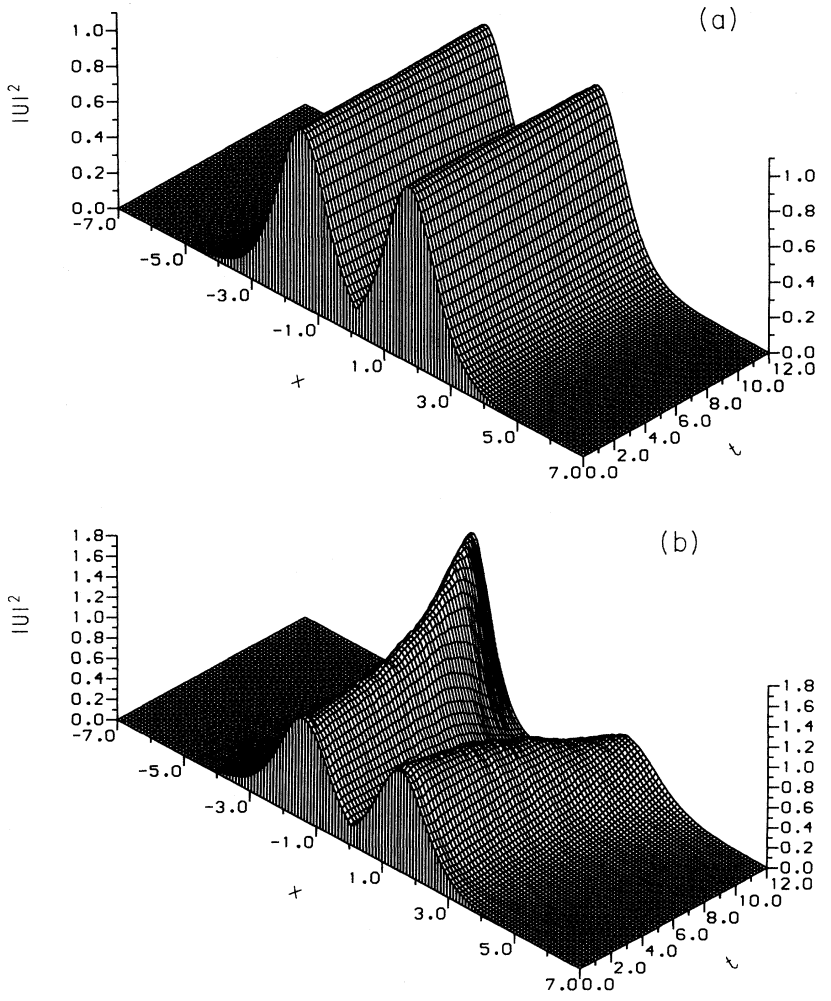

FIG. 5. (a) Evolution of a symmetric perturbation of the double-peak mode for the crystal data of Fig. 3. $\mu=0.89$ and the input function is $[\mathrm{sech}(x-x_1),\ x>0]$, $[\mathrm{sech}(x+x_1),\ x<0]$, where $x_1=1.1\ \tanh^{-1}(\mu)$. (b) Evolution of an asymmetric perturbation of the double-peak mode for the same crystal data. The input function is $[\mathrm{sech}(x-x_1)\ x>0]$, $[\mathrm{sech}(x+x_2),\ x<0]$, where $x_1=0.95\ \tanh^{-1}(\mu)$, $x_2=1.05\ \tanh^{-1}(\mu)$, and $\mu=0.89$.

matter what the symmetry is. In the next section, the stationary states and stability tests will be produced numerically.

V. NUMERICAL ANALYSIS

The nonlinear envelope equation (10) will now be solved numerically, not only to check the existence of the single peak and double peak solutions, but to check the analytical stability conclusions of the previous section. For numerical purposes, the delta function is defined as $\delta(x) = (1/\sqrt{\varepsilon\pi})\exp(-x^2/\varepsilon)$, where ε is taken to be as small as is consistent with numerical convergence, e.g., typically, $\varepsilon = 5\times 10^{-3}$. The modified nonlinear Schrödinger equation (9) is actually solved, here, using a beam propagation method, for various types of input conditions.

The data for all the figures are $D_0/a = 4$. The transverse length scale is measured in units of $D_0 = 4a = 1.6$ nm, the time scale is measured in units of $2D_0^2 m\omega_m/(a^2 k_2) = 0.16$ ps, and the modulus of the amplitude is measured in units of ψ_m. For each case, ψ_m^2 satisfies the threshold condition for the existence of the solitonlike localized state. The excitations are allowed to evolve sufficiently, in time, for stationary states to be assured, or for any perturbations to expose stability, or instability. The data selected are merely typical, and possible, for the purposes of illustration. $|(m-M)/m| = 0.1$ is used, which means that $M/m = 0.9$. This figure could correspond to P in Si, or Mg in Si. From $x_0 = \tanh^{-1}(\mu)$, the dimensionless $|x_0|$ used in these calculations is 1.42.

Using a Lennard-Jones potential, from which the second and fourth derivatives, evaluated at the minimum position, yield k_2 and k_4 leads to

$$\frac{\psi_m}{a} \approx 2.12\times 10^{-2}\frac{1}{(D_0/a)}. \tag{32}$$

This can be compared with the thermal mean square displacement, which is estimated to be $\langle u^2\rangle \cong (k_B T)/k_2$, where k_B is Boltzmann's constant and T is the absolute temperature. For $T = 300$ K, for example, $\sqrt{\langle u^2\rangle}/a \approx 10^{-2}$. Figure 2 is a plot of ψ_m/a against (D_0/a) and it also shows the estimated value of $\sqrt{\langle u^2\rangle}/a$. This very simple demonstration of the threshold condition for the localized state reveals that, resting upon the estimates given here, the soliton threshold for $D_0/a = 4$ lies *below* the room temperature thermal line.

The single peak and double peak exact solutions propagate without change of shape. On the other hand, Fig. 3 shows the evolution, with time, of an initial state that has the form sech(x). It is quite interesting, to see how this *nonexact* input shape propagates in time. Figure 3(a) shows that, for $\mu < 0$, a sech(x) input evolves to take on the appearance of the single peak solution. For $\mu > 0$, Fig. 3(b) shows that using a sech(x) input form is rather a severe test. The final stationary state here ought to be the double peak structure. This, clearly, does not appear to be happening and the explanation is that such an input is equivalent to "squashing" the two peaks together, thereby creating a strong repulsive potential. This repulsion not only forces the peaks apart, but also imparts "momentum." Hence, instead of settling onto a double peak, stationary, state, the two peaks continue to "fly apart," each with a finite velocity.

The next set of computer experiments is devoted to an investigation of the stability. First, the evolution of the single-peak mode, subjected to either a symmetric, or antisymmetric, perturbation, is studied. In the unperturbed state, the single peak structure is defined as sech$(|x|-x_0)$. The symmetric perturbed state is created by shifting the value of x_0 to $1.1x_0$ (larger shifts achieve only the same effect). An antisymmetric perturbation is achieved by using sech $(x-x_1)$ $[x>0]$ and sech$(x+x_2)$ $[x<0]$, with $x_1 = 0.95x_0$ and $x_2 = 1.05x_0$. For both types of perturbation, a good single peak stationary state evolves after 12 time units have elapsed but, naturally, an asymmetric perturbation takes longer to evolve. This is demonstrated by the noise on the surface plot in Fig. 4. The second set of stability plots concerns the double-peak structure. This double peak structure is immune [Fig. 5(a)] to the symmetric perturbation, but Fig. 5(b) shows that it is dramatically broken up by an asymmetric perturbation

ACKNOWLEDGMENTS

This work was supported in part by NSF Grants No. DMR-9319404 and No. INT-9224574. The authors A.D.B. and K.X. also acknowledge support from the U.K. Engineering and Physical Sciences Research Council (EPSRC).

[1] A. J. Sievers and S. Takeno, Phys. Rev. Lett. **61**, 970 (1980).
[2] F. Fisher, Ann. Phys. (N.Y.) **2**, 296 (1993).
[3] A. M. Kosevich and A. S. Kovalev, Zh. Éksp. Teor. Fiz. **67**, 1793 (1974) [Sov. Phys. JETP **40**, 891 (1974)].
[4] A. S. Dolgov, Fiz. Tverd. Tela (Leiningrad) **28**, 1641 (1986) [Sov. Phys. Solid State **28**, 907 (1986)].
[5] J. B. Page, Phys. Rev. B **41**, 7835 (1990).
[6] S. Takeno, J. Phys. Soc. Jpn. **59**, 3861 (1990).
[7] S. R. Bickham, S. A. Kiselev, and A. J. Sievers, Phys. Rev. B **47**, 14 206 (1993).
[8] S. A. Kiselev, S. R. Bickham, and A. J. Sievers, Phys. Rev. B **48**, 13 508 (1993).
[9] Y. S. Kivshar, Phys. Lett. A **161**, 80 (1991).
[10] F. W. Montroll and R. B. Potts, Phys. Rev. **100**, 525 (1955).
[11] G. P. Agrawal, *Nonlinear Fiber Optics* (Academic, Boston, 1989).
[12] G. B. Whitham, *Linear and Nonlinear Waves* (Wiley, New York, 1974).